Table 2. Analytical data of Ni(II) and other metal ions separated in Figure 3

Metal ions, added	Added amount (mg/50 mL)	Recovered amount (mg)	Found* (mg)
Pb(II)	2.0	0.994	1.97
Co(II)	2.0		2.03
Zn(II)	2.0		1.98
Fe(II)	2.0		1.99

*Values agreed with a precision of ±1.5%. amount of Ni(II) taken, 1.0 mg/50 mL.

with silica-dimethylglyoxime adsorbent. The results indicate that this adsorbent can act as an effective adsorbent for preconcentration of the Ni(II) ion.

Separation of Ni(II). The separation of trace amounts of Ni(II) from other metal ions was examined by column method. The 50 mL sample solution containing 1 mg Ni(II), each 2 mg of Co(II), Fe(II), Pb(II) and Zn(II) was loaded through the column (3.14 $cm^2 \times 5$ cm) at a rate 0.5 mL and eluted with 0.1 M HCl eluent. The results is Figure 3, in which Ni(II) is separation from Co(II), Fe(II), Pb(II) and Zn (II). The recoveries of Ni(II) and the added ions were above 98.5% (Table 2).

References

1. Mahmoud, M. E.; Soliman, E. M. *Talanta* **1997**, *44*, 1063.
2. D'yachenko, N. A.; Trofimchuk, A. K.; Sukhan, V. V. *Journal of Analytical Chemistry* **1995**, *50*, 772.
3. Gushikem, Y.; Ehirim, E. O. *Talanta* **1995**, *42*, 1625.
4. Sarkar, A. R.; Datta, P. K.; Sarkar, M. *Talanta* **1996**, *43*, 1857.
5. Alimarin, I. P.; Tikhomirova, T. I. *Talanta* **1987**, *34*, 103.
6. Sturgeon, R. E.; Berman, S. S.; Willie, S. N.; Desaulniers, J. A. *Anal. Chem.* **1981**, *53*, 2337.
7. Tong, A.; Atman, O. Y.; Howard, A. G. *Analyst* **1987**, *115*, 947.
8. Moriera, J. C.; Gushikem, Y. *Anal. Chim. Acta* **1985**, *176*, 263.
9. Tong, A.; Akama, Y.; Tanaka, S. *Analyst* **1990**, *230*, 179.
10. Mahmoud, M. E. *Anal. Lett.* **1996**, *29*, 1791.
11. Simonzadeh, N.; Schilt, A. A. *Talanta* **1988**, *35*, 187.
12. Pyell, U.; Stork, G.; Fresenius, Z. *Anal. Chem.* **1992**, *343*, 576.
13. Guedas, M. M.; Rmer, F. G.; Griepenik, B. *Anal. Chem.* **1977**, *287*, 19.
14. Jeffery, G. H. *Textbook of Quantitative Chemical Analysis*; Longman, U.K., 1989; pp 462-463.

Preparation and Electrical Properties of Delafossite-Type Oxides $AgNi_{1-x}Fe_xO_2$ ($0 \leq x \leq 0.5$)

Yu-Ju Shin*, Ji-Hyun Kwak, and Don Kim†

Department of Chemistry, the Catholic Univ. of Korea, Buchon-si, Kyeongki-do 420-743, Korea
†Department of Chemistry, Pukyong National University, Nam-gu, Pusan 608-737, Korea

Received December 16, 1997

Delafossite-type oxides $A^{I}B^{III}O_2$ (A=Cu, Ag, Pt, Pd; B=Fe, Co, Ni, Cr, Rh....)[1,2] have distinctive features due to their two-dimensional structure and the existence of two kinds of transition metals that occupy different crystallographic sites. Trivalent B cations are octahedrally coordinated by oxides and these octahedral units share edges leading to planar $[BO_2]^-$ slabs, which are stacked along *c* axis. Monovalent A cations are located in the linear sites furnished with $[BO_2]^-$ slabs, and form hexagonal planar array in *ab* plane. Delafossite-type oxides crystallize in various polytypes according to the stacking way along *c* axis.[2] Among them, the type 3R is represented in Figure 1. The electronic transport properties of delafossite-type compounds had been known to depend primarily on the electronic configuration of A-site ions: With d^{10} as Ag^+ or Cu^+ they become semiconductors, otherwise metallic as are $PdCrO_2$ and $PtCoO_2$. This correlation was rationalized by Rogers *et al.*, by using a schematic MO diagram of $[AgO_2]^{3-}$ cluster.[3] However, semimetallic properties of $AgNiO_2$ were reported[4,5] later. In this case both NiO_2 and hexagonal Ag sublattices were considered for the electronic structure, and charge carriers were generated through a slight overlap of Ag 4d and σ^*(Ni-O) bands (Figure 2). The substitution effects on the electrical transport properties have been studied with a solid solution system $AgNi_{1-x}Co_xO_2$ by one of us[6]: a metal-insulator transition was found around x_c=0.3 and the band overlap disappears for $x \geq 0.4$. However, further works on the substitution effects seemed necessary to get more general understanding about the band overlap of $AgNiO_2$. For this purpose, we report here the synthesis of new solid solutions $AgNi_{1-x}Fe_xO_2$ ($0 \leq x \leq 0.5$) and their electrical transport properties.

Experimental

Samples were prepared by cation-exchange reaction,[7,8] using precursors of $NaNi_{1-x}Fe_xO_2$, which were obtained by heating the mixtures of Na_2O, NiO and Fe_2O_3 at 600-700 °C under O_2 atmosphere for 14-18 hrs. Each of $NaNi_{1-x}Fe_xO_2$ samples was crystallized in single phase with α-$NaFeO_2$ structure (R3m) for $0 \leq x \leq 0.5$, but bi-phased with x>0.5 with the appearance of $NaFeO_2$, even at higher reaction tem-

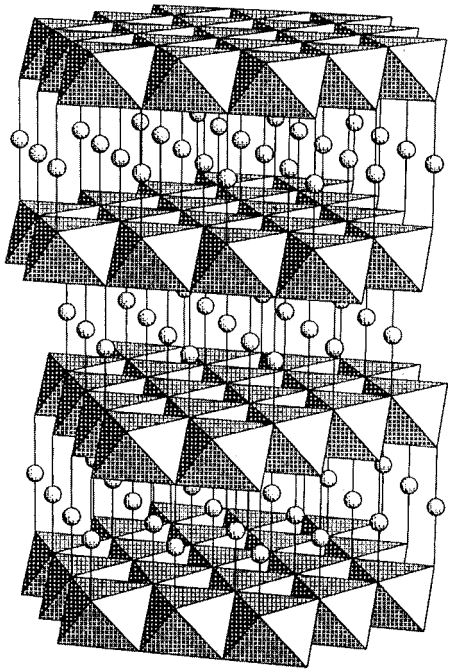

Figure 1. 3R-type delafossite structure of ABO_2 oxides. Balls represent the A^1 ions.

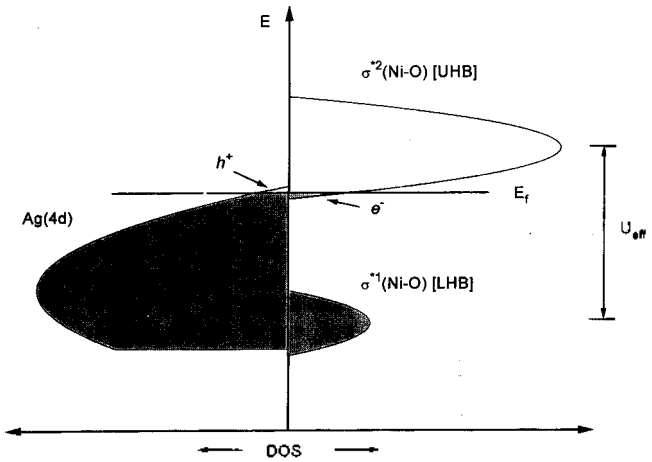

Figure 2. Schematic energy diagram of $AgNiO_2$. The antibonding orbital σ^*(Ni-O) is separated into two bands, a fulfilled lower Hubbard band (LHB) and a empty upper Hubbard band (UHB) due to the effective intraatomic repulsion energy Ueff. The UHB σ^{*2} (Ni-O) overlaps with Ag 4d band, generating electrons and holes respectively in each band.[4]

perature. Cation-exchange reactions were carried out by heating the mixtures of $NaNi_{1-x}Fe_xO_2$ and $AgNO_3$ in vacuum-sealed pyrex tubes at 300-350 °C for 7-10 days. Excessive $AgNO_3$ was used to facilitate the reaction and KNO_3 was added to prevent the eventual reduction of Ag^+ to Ag^0. Products were recovered by washing out the remnant nitrates with distilled water or absolute ethanol, and finally greyish-black powders were obtained after vacuum-drying. The lattice parameters were determined by least-square method from the powder X-ray diffractograms. Electrical resistivity was measured using conventional 4-probe method with silver paste contact over each sample at the temperature range of 10-300 K. Thermoelectric power (seebeck coefficient) measurement was carried out by using an automated temperature relaxation method[9,10] at the range of 75-300 K.

Results and Discussion

Powder X-ray diffraction measurements showed all the $AgNi_{1-x}Fe_xO_2$ samples exhibit 3R-type delafossite structure (R3m). This may reflect the dependency of structure of product on the used precursor, which is of type O3 in this work.[8] We could not detect any extra diffraction peaks suggesting the eventual ordering of Ni^{3+} and Fe^{3+} ions, so they are considered to be statistically distributed in B-site. Solid solution domain was $0 \leq x \leq 0.5$, as pre-determined in Na-phases. Lattice parameters a_H and c_H (hexagonal setting) show a gradual increase with x (Figure 3). It may be simply attributed to the large difference of ionic radii between Ni^{3+} (0.56 Å) and Fe^{3+} (0.645 Å : HS). This also ensures the high-spin state of Fe^{3+}, otherwise the lattice parameters would not be increased (Fe^{3+}: 0.55 Å : LS).[11] The increase of lattice parameters would designate that the average distance of Ni-O bond is increased and consequently its decreasing of covalency. The thermal variation of electrical resistivity is represented in Figure 4. As x increases, the resistivity increases gradually and a metal-insulator transition has occurred around x_c=0.1 (Figure 4(b)). Figure 5 shows the variation of the thermoelectric power of α some $AgNi_{1-x}Fe_xO_2$ solid solutions as a function of temperature. For $AgNiO_2$, α is positive at low temperature and changes its sign around 250 K as already reported.[5,6] The switching temperature decreases with x, but the positive region still remains even in the insulating phases (x=0.3), though α becomes more and more negative as x increases. Since the positive α is due to

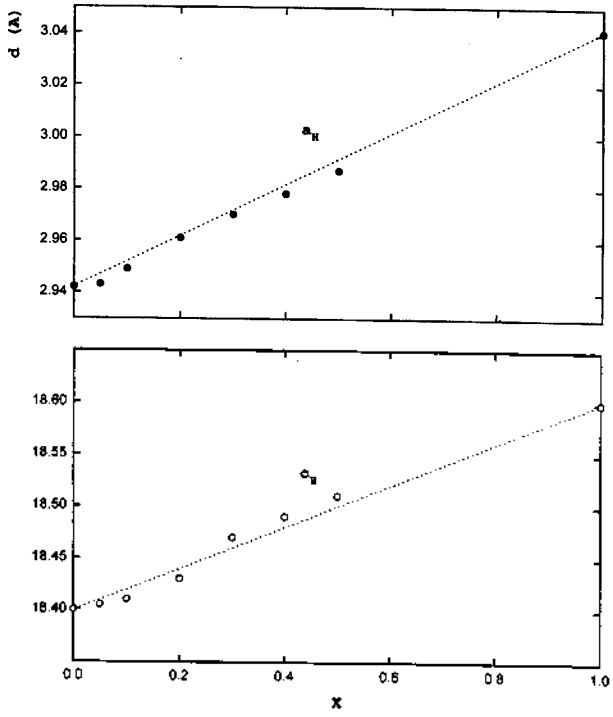

Figure 3. Evolution of lattice parameters aH and cH of $AgNi_{1-x}Fe_xO_2$. Those of $AgFeO_2$ are also shown for comparison.

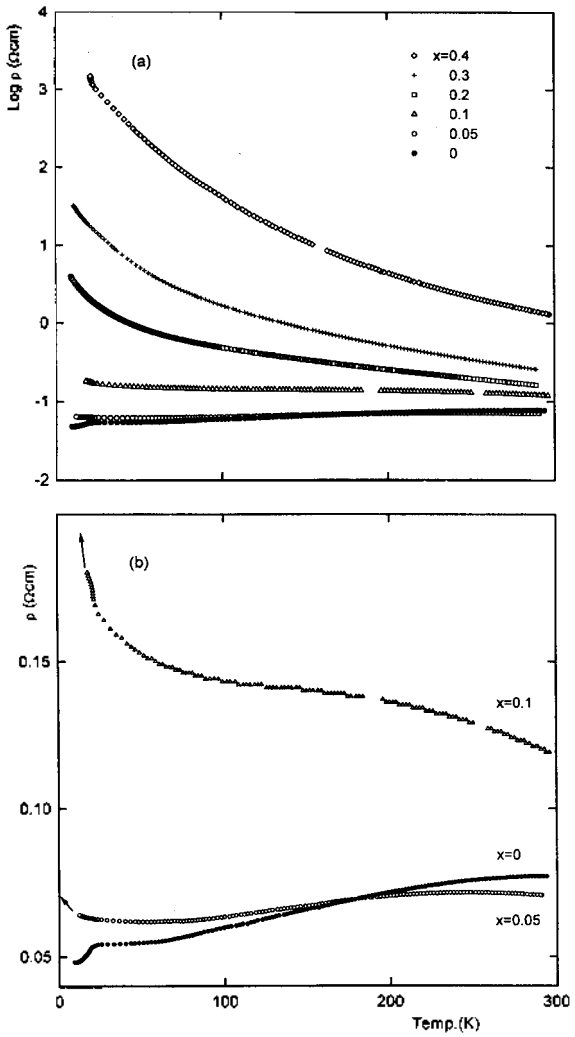

Figure 4. Thermal variation of resistivity of $AgNi_{1-x}Fe_xO_2$ represented in logarithm (a) and natural scale (b). A metal-insulator transition occurs around x_c=0.1, where the resistivity increases up to infinity as T approaches to 0 K.

the existence of band overlap,[5] such results imply that the band overlap did not completely disappear after the metal-insulator transition.

The overlap of Ag 4d and σ^*(Ni-O) bands in $AgNiO_2$ may be simply expressed by a chemical equilibrium $Ag^+ + Ni^{3+} \rightleftarrows Ag^{2+} + Ni^{2+}$, being largely shifted toward left-hand side. As a result, holes and electrons are created respectively in Ag and NiO_2 sublattices.[4,5] The carrier concentration must be very low, particularly in that the hole should be associated with Ag^{2+} which is not adequate for two-fold linear site. The substitution of Ni^{3+} by Fe^{3+} should give rise to several changes into the electronic structure. First of all, the decrease of Ni^{3+}-population in B site should lead to withdrawing of σ^*(Ni-O) band and the overlap becomes smaller so that the tendency of localization of carriers is increased. The random distribution of Fe^{3+} ions in B site should introduce the random potential into the lattice and hence localize the states near the band edges, giving rise to the band-tailing (Anderson localization[12]). This effect may retard the separation of two bands, however, whether the carriers are localized or not depends essentially on the

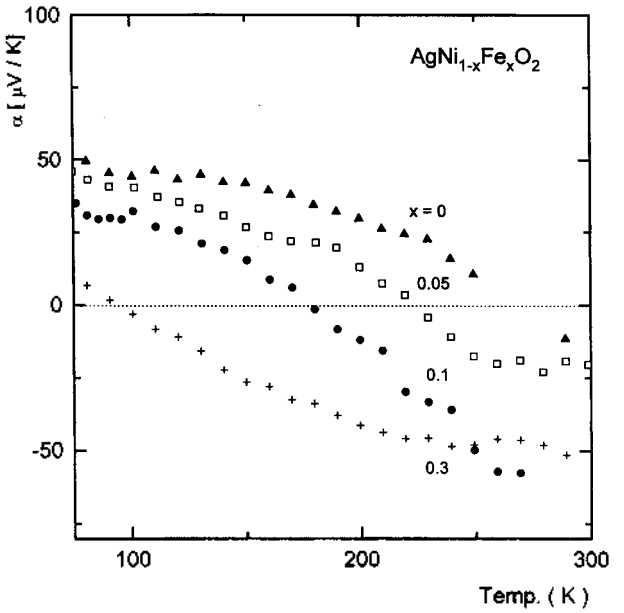

Figure 5. Thermal variation of thermoelectric power of $AgNi_{1-x}Fe_xO_2$.

relative position of the mobility-edge over Fermi level. The increase of lattice parameters with x strongly suggests the average bond distance of Ni-O is elongated. This implies that the covalency of Ni-O bond is weakened in substituted phases, so the σ^*(Ni-O) band is narrowed and, at the same time, would be shifted towards lower energy region. This process involves two competing effects on the charge carriers: Band narrowing would facilitate the localization, while the band shift may reinforce the overlapping.

As shown in Figure 5, the existence of charge carrier even in the insulating phases (x=0.3) implies that the transition in $AgNi_{1-x}Fe_xO_2$ should be considered as rather an Anderson-type than as band separation, as was already observed in $AgNi_{1-x}Co_xO_2$. According to the resistivity measurement, however, the onset of localization of carriers takes place more sensitively with Fe^{3+} (x_c=0.1) than Co^{3+} (0.3). This may be understood by considering mainly the two aspects: Anderson localization has been known to take place to a degree of perturbation on the periodic potential by the random potential,[12,13] which is primarily dependent on the difference of total ionization energies of host ion Ni^{3+} (IE_{total} $=IE_1+IE_2+IE_3$=60.97 eV) and the substituents, Fe^{3+} (54.70 eV) and Co^{3+} (58.42 eV).[14] The greater difference with Fe^{3+} (IE_{total}=6.27 eV) than with Co^{3+} (2.55 eV) should render the former more effective to localize the states near the Fermi-level. The second is related with the reduced covalency of Ni-O bond in Fe^{3+}-substituted phases. It should facilitate the localization process in contrast to the Co^{3+}-substituted phases where the Ni-O bonds are thought to be reinforced due to the decrease of lattice parameters with substitution ratio. From this point of view, the effect of the band shift seems less important than the band narrowing in $AgNiO_2$.

When both carriers-electrons and holes-are present at the same time, thermo-electric power α can be expressed as $\alpha = (\alpha_e\sigma_e + \alpha_h\sigma_h)/\sigma_{tot}$, where the subscripts e and h denote each contribution to the conductivity (σ_e, σ_h) and to the thermoelectric power (α_e, α_h), and $\sigma_{tot}=\sigma_e+\sigma_h$. The absolute

values of α_e and α_h are generally of a few tens of μV/K and proportional to T when Fermi level is situated in a band.[12] Therefore, the sign-change of α from + to − with temperature should be primarily attributed to the augmentation of σ_e/σ_{tot} as T increases. Such a tendency is apparently strengthened for the nonmetallic phases, in which carriers are considered to move *via* hopping process by the aid of lattice vibration. The mobility of electron seems to be more easily activated than hole, since the electrons are associated with Ni^{2+} ions and can move from sites to sites, keeping the local symmetry as octahedral for both Ni^{2+} and Ni^{3+}. But hopping of holes associated with Ag^{2+} ions would require a large change of local symmetry, from 4-fold rectangular (Ag^{2+}) to 2-fold linear (Ag^{+}).

In conclusion, $AgNi_{1-x}Fe_xO_2$ undergoes a metal-insulator transition through the Anderson localization process with relatively a small substitution ratio x_c=0.1 with respect to $AgNi_{1-x}Co_xO_2$, due to the large random potential introduced by Fe^{3+} ions and partly the reduced covalency of Ni-O bond.

Acknowledgment. This work was supported by the grant of (961-0306-057-2) from Korea Science and Engineering Foundation.

References

1. Pabst, A. *Amer. Mineral.* **1946**, *31*, 539.
2. Doumerc, J. P.; Ammar, A.; Wichainchai, A.; Pouchard, M.; Hagenmuller, P. *J. Phys. Chem. Solids* **1987**, *48*, 37.
3. Rogers, D. B.; Shannon, R. D.; Prewitt, C. T.; Gillson, J. L. *Inorg. Chem.* **1971**, *10*, 723.
4. Wichainchai, A.; Dordor, P.; Doumerc, J. P.; Marquestqut, E.; Pouchard, M.; Hagenmuller, P. *J. Solid State Chem.* **1988**, *74*, 126.
5. Shin, Y. J.; Doumerc, J. P.; Dordor, P.; Pouchard, M.; Hagenmuller, P. *J. Solid State Chem.* **1993**, *107*, 194.
6. Shin, Y. J.; Doumerc, J. P.; Dordor, P.; Delmas, C.; Pouchard, M.; Hagenmuller, P. *J. Solid State Chem.* **1993**, *107*, 303.
7. Shannon, R. D.; Rogers, D. B.; Prewitt, C. T. *Inorg. Chem.* **1971**, *10*, 713.
8. Shin, Y. J.; Kwak, J. H.; Yoon, S. *Bull. Kor. Chem. Soc.* **1997**, *18(7)*, 775.
9. Marcy, H. O.; Marks, T. J.; Kannewurf, C. R. *IEEE Trans. Instru. Meas.* **1990**, *39*, 756.
10. Kim, D.; Honig, J. M. *Phys. Rev. B* **1994**, *49*, 4438.
11. Shannon, R. D. *Acta Crystallogr.* **1976**, *A32*, 751.
12. Mott, N. F. *Metal-Insulator Transitions*; Taylor and Francis: London, 1991.
13. for example, Mott, N. F.; Kaveh, M. *Adv. Phys.* **1985**, *34*, 329.
14. Bowser, J. R. *Inorganic Chemistry*; Brooks/Cole: Belmont, 1993.

Synthesis and X-Ray Crystal Structure of Copper(II) Complex with Chiral Tetradentate N_4 Mono Amide Ligand, 2(S)-2,9-diamino-4,7-diazanonane-3-one(S-aladienH)

Bae-Wook Lee, Dong-Yeub Kim†, Bok-Jo Kim, Chang-Eon Oh, Bong-Gon Kim‡, and Myung-Ki Doh*

Department of Chemistry, Yeungnam University, Kyongsan 712-749, Korea
†Department of Chemical Industry, Yeungnam Junior College, Taegu 705-037, Korea
‡Department of Chemical Education, Kyeongsang National University, Chinju 660-701, Korea
Received January 20, 1998

Transition metal complexes of chelating ligands containing an amide functional group have received much attention as a result of a marked increase in the lability of amide portion.[1] Many investigations have revealed that the deprotonated nitrogen of organic amides donates to metal ions, stabilizing high oxidation states. Several examples of deprotonated bis-amides with the picolinamide unit as a basic component have been shown to act as tetradentate N_4 ligands.[2] The bis-picolinamide ligands, *N,N'*-bis(2'-pyridinecarboxamide)-*cis*-1,2-cyclohexane(*cis*-bpch),[2a] *N,N'*-bis(2'-pyridinecarboxamide)-*trans*-1,2-cyclohexane(*trans*-bpch),[2b] *N,N'*-bis(2'-pyridinecarboxamide)-1,2-benzene($bpbH_2$)[2c] and *N,N'*-bis(6'-methylpyridine-2'-carboxamido)-1,2-benzene(6-me$bpbH_2$)[2d] have a pronounced tendency for planar N_4 tetradentate coordination to Cu(II) ion on deprotonation. They have been shown to take stereochemistries of a distorted square-pyramid. However, few Cu(II) complexes have tetradentate chiral mono amide functionality. On the other hand, edda(ethylenediaminediacetato) type ligands seem to have a certain characteristic of hardly coordinating with metal ions in a plane.[3]

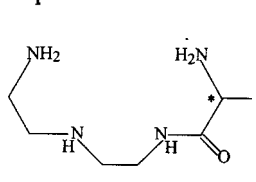

S-aladienH

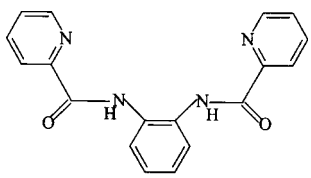

$bpbH_2$

Thus, in this study we described the synthesis, spectral properties and X-ray crystal structure of $[Cu(S\text{-aladien})H_2O]^+$ with chiral tetradentate mono amide ligand, 2(*S*)-2,9-